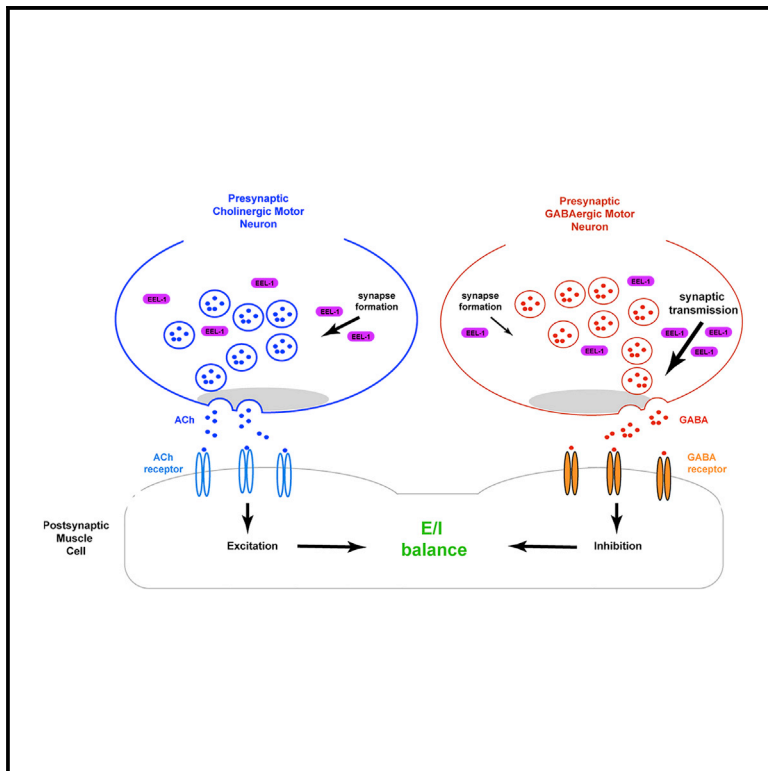


## The HECT Family Ubiquitin Ligase EEL-1 Regulates Neuronal Function and Development

### Graphical Abstract



### Authors

Karla J. Opperman, Ben Mulcahy, Andrew C. Giles, ..., Ken Dawson-Scully, Mei Zhen, Brock Grill

### Correspondence

bgrill@scripps.edu

### In Brief

Genetic changes in the HECT ubiquitin ligase EEL-1/HUWE1 are associated with intellectual disability. Using *C. elegans*, Opperman et al. show that EEL-1/HUWE1 is required for GABAergic presynaptic transmission and excitatory/inhibitory (E/I) transmission balance. These findings have potentially important implications for the link between HUWE1 and intellectual disability.

### Highlights

- GABAergic presynaptic transmission is impaired in *eel-1* mutants
- EEL-1 is required for E/I balance in the worm motor circuit
- Locomotion and electroshock responses are abnormal in *eel-1* mutants
- EEL-1 functions within the RPM-1 signaling pathway to regulate neuronal development



# The HECT Family Ubiquitin Ligase EEL-1 Regulates Neuronal Function and Development

Karla J. Opperman,<sup>1</sup> Ben Mulcahy,<sup>2</sup> Andrew C. Giles,<sup>1</sup> Monica G. Risley,<sup>4</sup> Rayna L. Birnbaum,<sup>1,5</sup> Erik D. Tulgren,<sup>6</sup> Ken Dawson-Scully,<sup>4</sup> Mei Zhen,<sup>2,3</sup> and Brock Grill<sup>1,7,\*</sup>

<sup>1</sup>Department of Neuroscience, The Scripps Research Institute, Scripps Florida, Jupiter, FL 33458, USA

<sup>2</sup>Lunenfeld-Tanenbaum Research Institute, Mount Sinai Hospital, Toronto, ON M5G 1X5, Canada

<sup>3</sup>Department of Molecular Genetics and Physiology, University of Toronto, Toronto, ON M5S 1A8, Canada

<sup>4</sup>Department of Biological Sciences, Florida Atlantic University, Boca Raton, FL 33431, USA

<sup>5</sup>Harriet L. Wilkes Honors College, Florida Atlantic University, Jupiter, FL 33458, USA

<sup>6</sup>Department of Pharmacology, University of Minnesota, Minneapolis, MN 55455, USA

<sup>7</sup>Lead Contact

\*Correspondence: [bgrill@scripps.edu](mailto:bgrill@scripps.edu)

<http://dx.doi.org/10.1016/j.celrep.2017.04.003>

## SUMMARY

Genetic changes in the HECT ubiquitin ligase *HUWE1* are associated with intellectual disability, but it remains unknown whether *HUWE1* functions in post-mitotic neurons to affect circuit function. Using genetics, pharmacology, and electrophysiology, we show that EEL-1, the *HUWE1* ortholog in *C. elegans*, preferentially regulates GABAergic presynaptic transmission. Decreasing or increasing EEL-1 function alters GABAergic transmission and the excitatory/inhibitory (E/I) balance in the worm motor circuit, which leads to impaired locomotion and increased sensitivity to electroshock. Furthermore, multiple mutations associated with intellectual disability impair EEL-1 function. Although synaptic transmission defects did not result from abnormal synapse formation, sensitizing genetic backgrounds revealed that EEL-1 functions in the same pathway as the RING family ubiquitin ligase RPM-1 to regulate synapse formation and axon termination. These findings from a simple model circuit provide insight into the molecular mechanisms required to obtain E/I balance and could have implications for the link between *HUWE1* and intellectual disability.

## INTRODUCTION

GABA ( $\gamma$ -aminobutyric acid) is the principal inhibitory neurotransmitter in the mammalian brain and in the simple motor circuit of the nematode *C. elegans*. In both cases, inhibition by GABA is necessary to achieve a balance of excitatory and inhibitory transmission that is required for proper circuit function and behavior (Gatto and Broadie, 2010; Zhen and Samuel, 2015). Imbalances in the excitatory/inhibitory (E/I) ratio is a central feature of many neurodevelopmental disorders, including autism, epilepsy, and intellectual disability (Gatto and Broadie, 2010; Rubenstein and Merzenich, 2003).

The motor circuit of *C. elegans* relies on a precise balance of cholinergic excitation and GABAergic inhibition of body wall muscles to generate locomotion (Zhen and Samuel, 2015). This model circuit has been tremendously useful for understanding the molecular mechanisms of presynaptic transmission (Barclay et al., 2012). Recent studies have begun to explore the molecular mechanisms that regulate E/I balance in the worm motor circuit, which remain poorly understood (Cherra and Jin, 2016; Jospin et al., 2009; Kowalski et al., 2014; Stawicki et al., 2011; Vashlishan et al., 2008). Over the past decade, this simple circuit has also emerged as a valuable tool for understanding the molecular and cellular mechanisms that affect neurodevelopmental disorders such as epilepsy and autism (Bessa et al., 2013).

The *HECT*, *UBA* and *WWE domain-containing protein 1* (*HUWE1*) is a homologous to E6AP c-terminus domain (HECT) family ubiquitin ligase with growing genetic links to intellectual disability. Increased copies of *HUWE1* are associated with non-syndromic intellectual disability (Friez et al., 2016; Froyen et al., 2008, 2012; Madrigal et al., 2007). Missense mutations in *HUWE1* occur in multiple families with intellectual disability, including families with Juberg-Marsidi-Brooks syndrome (Friez et al., 2016; Froyen et al., 2008; Isrie et al., 2013). This suggests that both increased and decreased *HUWE1* function could be associated with intellectual disability, but evidence from an in vivo model system supporting or refuting this possibility remains absent.

Huwe1 functions in early development of the nervous system by regulating neural progenitor proliferation and differentiation (Forget et al., 2014; Zhao et al., 2008). This function of Huwe1 is critical for laminar patterning of the cortex (Zhao et al., 2009). In the hippocampus, Huwe1 regulates neural stem cell quiescence (Urbán et al., 2016). Huwe1 also ubiquitinates and degrades Mitofusin, an important regulator of mitochondrial fusion (Leboucher et al., 2012). In *C. elegans*, there is a single ortholog of *HUWE1* called enhancer of EFL mutant phenotype 1 (EEL-1), which has primarily been studied in embryonic development (Page et al., 2007). EEL-1 was recently shown to affect neuroblast migration, indicating that EEL-1 and Huwe1 are conserved regulators of neural progenitors (de Groot et al., 2014).

Whether Huwe1 or EEL-1 have roles in post-mitotic neurons, affect synaptic transmission, or impact circuit function remains largely unexplored. Given mounting genetic evidence linking *HUWE1* and intellectual disability, addressing these issues using model circuits has become increasingly necessary. Experiments in worms and flies hinted at expanded functions for EEL-1 and HUWE1 in the nervous system beyond early development. A *C. elegans* RNAi screen with the drug aldicarb, a pharmacological inhibitor of acetylcholinesterase, implicated EEL-1 in neuronal function at the neuromuscular junction (NMJ) (Sieburth et al., 2005). In flies, ectopic expression of human HUWE1 results in aberrant axon branch formation in the dorsal cluster neurons (Vandewalle et al., 2013).

We have explored the function of EEL-1 using the motor circuit of *C. elegans*. Our results indicate that EEL-1 is expressed broadly in the nervous system, including both the excitatory cholinergic and inhibitory GABAergic motor neurons, but preferentially affects presynaptic GABAergic transmission. Reduced GABAergic transmission in *eel-1* mutants impairs locomotion and increases sensitivity to electroshock-induced paralysis, which can be reversed by the anticonvulsant drug retigabine. Furthermore, decreasing or increasing EEL-1 function causes opposing effects on GABAergic transmission. These observations suggest that EEL-1 is required to obtain E/I balance in a simple, well defined model circuit. Although defects in GABAergic transmission are not due to failed synapse formation, analysis of different types of neurons with sensitizing genetic backgrounds uncovered a less prominent EEL-1 function in synapse formation and axon termination. Our results indicate that *eel-1* functions in the same genetic pathway as the *regulator of presynaptic morphology 1* (*rpm-1*), an intracellular signaling hub and RING family ubiquitin ligase that regulates synapse and axon development (Grill et al., 2016). These findings expand our understanding of how EEL-1 functions in the nervous system and indicate that EEL-1 regulates GABAergic presynaptic transmission and is required for E/I balance in a simple model circuit.

## RESULTS

### Both Decreased and Increased EEL-1 Activity Alter Motor Neuron Function

The *C. elegans* motor circuit uses acetylcholine (ACh) as an excitatory neurotransmitter. The cholinergic motor neurons innervate the body wall muscles and stimulate muscle contraction. GABA is the inhibitory transmitter in the worm motor circuit, and GABAergic motor neurons stimulate muscle relaxation. Locomotion is thought to arise from cholinergically mediated contraction and GABA-induced relaxation on opposing sides of the animal (Zhen and Samuel, 2015).

The acetylcholinesterase inhibitor aldicarb is a classic pharmacological assay of motor neuron function (Barclay et al., 2012). Application of aldicarb to an animal reduces ACh hydrolysis in the synaptic cleft of the NMJ. This leads to ACh accumulation, overstimulation of ACh receptors on muscles, and eventual paralysis. Previous studies identified RNAi targets and mutants that are resistant to inhibitors of cholinesterase (Ric) (Miller et al., 1996; Sieburth et al., 2005) and mutants that are hypersensitive to inhibitors of cholinesterase (Hic) (Loria et al., 2004; Vash-

lishan et al., 2008). The Ric phenotype is often caused by a reduction in ACh exocytosis leading to delayed paralysis. In contrast, two types of impairments can result in Hic phenotypes: enhanced ACh release from cholinergic motor neurons, resulting in more rapid paralysis, and reduced inhibitory GABAergic transmission to muscles, which causes E/I imbalance and more rapid paralysis.

The Kaplan lab previously showed that feeding animals bacteria expressing *eel-1* RNAi results in a moderate Ric phenotype (Sieburth et al., 2005). Using the same RNAi-sensitizing genetic background, *eri-1; lin-15B*, we observed similar results (Figures 1B and 1C). In contrast, *eel-1* RNAi resulted in the opposing phenotype, hypersensitivity to aldicarb, when a higher-sensitivity RNAi strain, *uls57; lin-15B*, was used (Figures 1D and 1E; Calixto et al., 2010).

To address these contradictory findings with RNAi, we tested two *eel-1* null mutants, *ok1575* and *zu462* (Figure 1A). Both *eel-1* mutants were hypersensitive to aldicarb (Figures 1F and 1G). This phenotype was rescued by transgenic expression of EEL-1 using a native *eel-1* promoter or pan-neuronal promoter but not with expression of the negative control GFP (Figures 2A and 2B). Thus, expression of EEL-1 in neurons is sufficient to rescue hypersensitivity to aldicarb caused by *eel-1* (lf).

Because increased cholinergic or reduced GABAergic function results in a Hic phenotype, we tested cell-specific promoters for rescue. Expression of EEL-1 with a GABAergic motor neuron promoter rescued aldicarb hypersensitivity in *eel-1* mutants (Figures 2C and 2D). Rescue did not occur with promoters for the cholinergic motor neurons or muscles (Figures 2C and 2D).

We noted in rescue experiments that a subset of transgenic arrays, which can have variable levels of expression, showed resistance to aldicarb (Figure S1). Therefore, we tested how aldicarb responses are affected by transgenic overexpression of EEL-1 in wild-type animals. As shown in Figures 2E and 2F, overexpression of EEL-1 using a pan-neuronal driver caused mild resistance to aldicarb (Figures 2E and 2F). Overexpression with a GABAergic promoter also resulted in aldicarb resistance. In contrast, overexpression of negative control proteins (GFP or mCherry) had no effect.

These results show that loss and gain of EEL-1 function in GABAergic motor neurons produces opposing aldicarb effects. Thus, EEL-1 is both necessary and sufficient for the aldicarb response. These results are consistent with EEL-1 being required to achieve E/I balance in the motor circuit.

### EEL-1 Regulates Presynaptic Transmission in GABAergic Motor Neurons

To explore the physiological mechanism underpinning EEL-1 effects on the aldicarb response, we turned to electrophysiology. To isolate GABAergic function, we recorded neuromuscular transmission by patch-clamping muscle cells in the presence of tubocurarine, an ACh receptor blocker (Richmond and Jorgensen, 1999). *eel-1* mutants had reduced frequency of GABAergic miniature inhibitory postsynaptic currents (mIPSCs) (Figures 3A and 3B). mIPSC amplitude was mildly reduced in *eel-1* mutants (Figures 3A and 3B). mIPSC frequency defects were rescued by an integrated transgene, *bgg1s16*, that uses the native promoter to express EEL-1 (Figures 3C and 3D). Defects in mIPSC

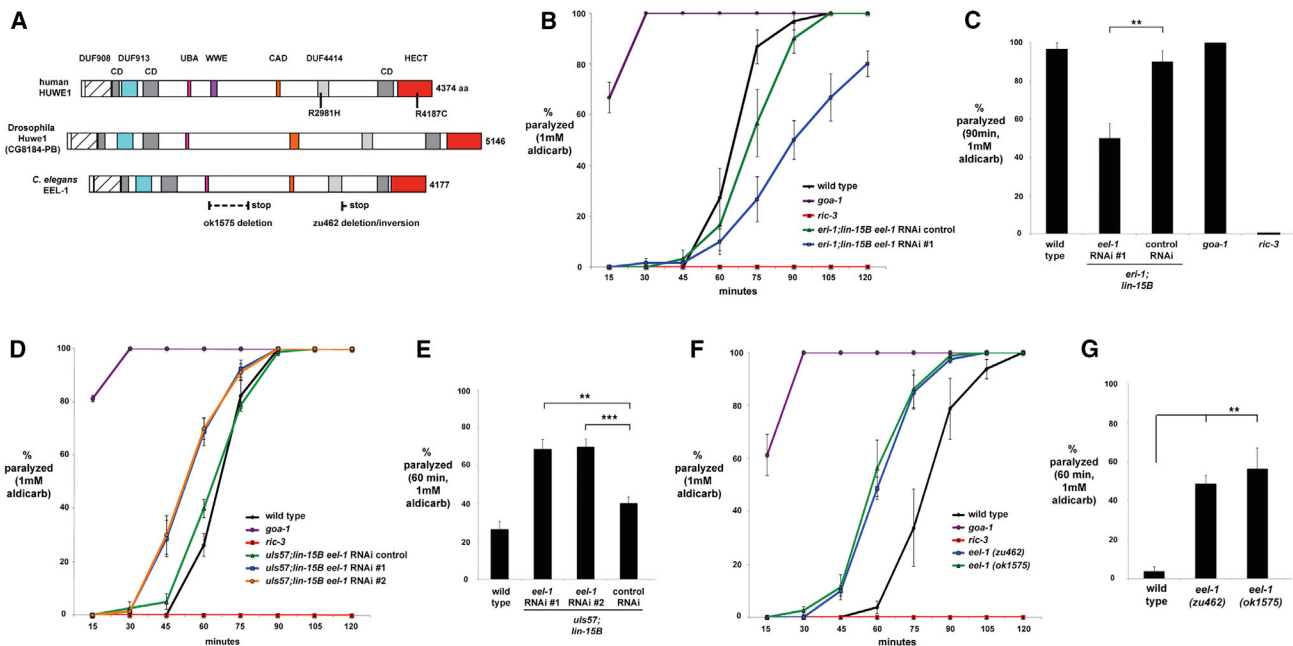


**Figure 1. *eel-1* RNAi and *eel-1* Mutations Cause Hypersensitivity to Aldicarb**

(A) Schematic of the human HUWE1, *Drosophila* Huwe1, and *C. elegans* EEL-1 protein sequences. Conserved mutations associated with intellectual disability (*R2981H* and *R4187C*) are highlighted. Deletions generated by *ok1575* and *zu462* are shown below. Conserved protein domains are annotated as follows: DUF, domain of unknown function, annotated in the NCBI conserved domain database; CD, conserved domain of unknown function, annotated here; UBA, ubiquitin-associated domain; WWE, WWE domain; CAD, conserved acidic domain; HECT, homologous to E6AP c-terminus domain.

(B) Aldicarb time course for *eel-1* RNAi using *eri-1; lin-15B* animals.

(C) Aldicarb paralysis at the 90-min time point for *eel-1* RNAi using *eri-1; lin-15B*.

(D) Aldicarb time course for *eel-1* RNAi using *uls57; lin-15B* animals.

(E) Aldicarb paralysis at the 60-min time point for *eel-1* RNAi using *uls57; lin-15B* animals.

(F) Aldicarb time course for *eel-1* mutants, *zu462*, and *ok1575*.

(G) Aldicarb paralysis at the 60-min time point for *eel-1* mutants. *goa-1* and *ric-3* mutants were included as positive controls for the Hic and Ric phenotypes. Significance was determined using an unpaired Student's t test, and error bars represent SEM. \*\**p* < 0.01, \*\*\**p* < 0.001.

amplitude trended toward rescue but were not significant (Figures 3C and 3D). These results indicate that EEL-1 is required for presynaptic GABAergic transmission but do not rule out the possibility of a modest effect on postsynaptic function.

To assess cholinergic transmission, analysis was done in the absence of the GABA receptor (UNC-49) to ensure that only excitatory cholinergic transmission was recorded. *unc-49; eel-1* mutants had no difference in cholinergic miniature excitatory postsynaptic current (mEPSC) frequency or amplitude compared with *unc-49* single mutants (Figures 3E and 3F). Therefore, EEL-1 regulates presynaptic transmission at the GABAergic, but not the cholinergic, NMJ.

### EEL-1 Is Expressed in the GABAergic Motor Neurons and Localizes to the Presynaptic Terminal

Our results with aldicarb pharmacology and electrophysiology indicate that EEL-1 regulates synaptic transmission in GABAergic motor neurons but not cholinergic motor neurons. To test whether this simply reflects *eel-1* expression patterns, we generated transgenic animals that express GFP using the *eel-1* promoter. *Peel-1::GFP* was observed in non-neuronal tissue (pharynx, intestine, and vulva; Figures S2A–S2C) and was strongly expressed in neurons, including numerous neurons in

the head (Figure 4A), motor neurons (Figures 4B and 4C), mechanosensory neurons (Figures 4D and 4E), HSN neurons (Figure S2D), and tail neurons (Figure S2E). GFP was detected in cholinergic (Figure 4B) and GABAergic motor neurons (Figure 4C). No expression was observed in muscle (data not shown). These results support our finding that EEL-1 regulates GABAergic transmission. Further, expression of *eel-1* in GABAergic and cholinergic motor neurons is consistent with EEL-1 being required to maintain E/I balance in the motor circuit. Broad *eel-1* expression in the nervous system leaves open the possibility that EEL-1 could regulate synaptic transmission in other types of neurons.

Next we analyzed the localization of EEL-1 in GABAergic motor neurons. We generated transgenic animals that simultaneously carry an integrated transgene that expresses Synaptobrevin-1::GFP and an extrachromosomal array that expresses mCherry::EEL-1. SNB-1::GFP and mCherry::EEL-1 were expressed with a GABAergic promoter. EEL-1 colocalizes with SNB-1 at the GABAergic presynaptic terminal (Figure 4F; Figure S3). EEL-1 was also observed in cell somata but not axon commissures (Figure S3). These results are consistent with EEL-1 functioning at the presynaptic terminal to regulate GABAergic transmission but do not exclude EEL-1 function in the soma.

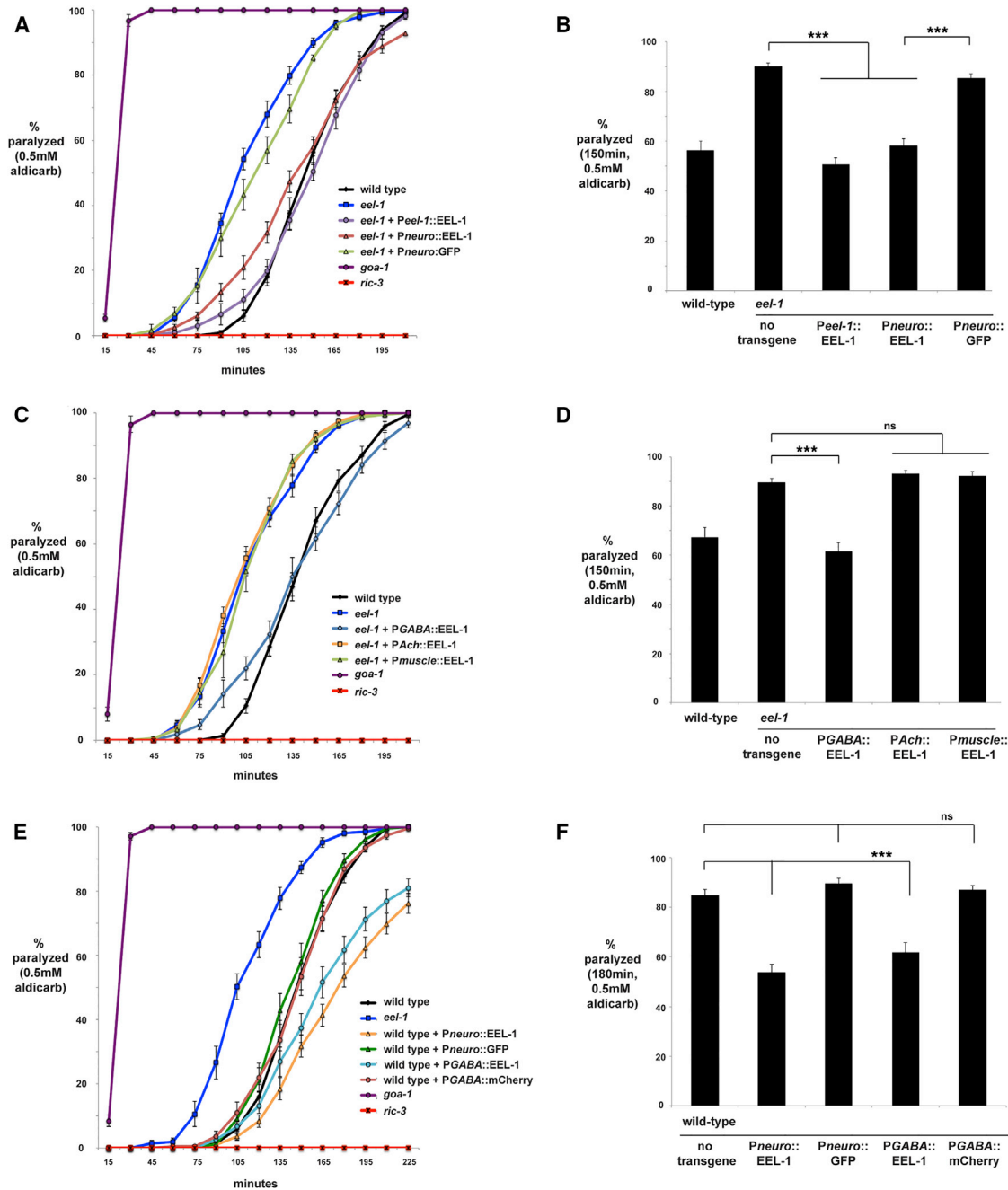


**Figure 2. EEL-1 Functions in GABAergic Motor Neurons to Regulate Aldicarb Hypersensitivity**

(A) Aldicarb time course showing that transgenic expression of EEL-1 rescues the aldicarb hypersensitivity of *eel-1* mutants.

(B) Aldicarb paralysis at the 150-min time point for EEL-1 transgenic rescues.

(C) Aldicarb time course showing that transgenic expression of EEL-1 in GABAergic motor neurons (*PGABA::EEL-1*) rescues the aldicarb hypersensitivity of *eel-1* mutants.

(D) Aldicarb paralysis at the 150-min time point for EEL-1 rescue in GABAergic motor neurons.

(E) Aldicarb time course showing that transgenic overexpression of EEL-1 in wild-type animals using a pan-neuronal promoter (*Pnuro::EEL-1*) or a promoter specific for GABAergic motor neurons (*PGABA::EEL-1*) results in resistance to aldicarb.

(F) Aldicarb paralysis at the 180-min time point for transgenic overexpression of EEL-1.

Significance was determined using an unpaired Student's t test, and error bars represent SEM. \*\*\*p < 0.001. ns, not significant.

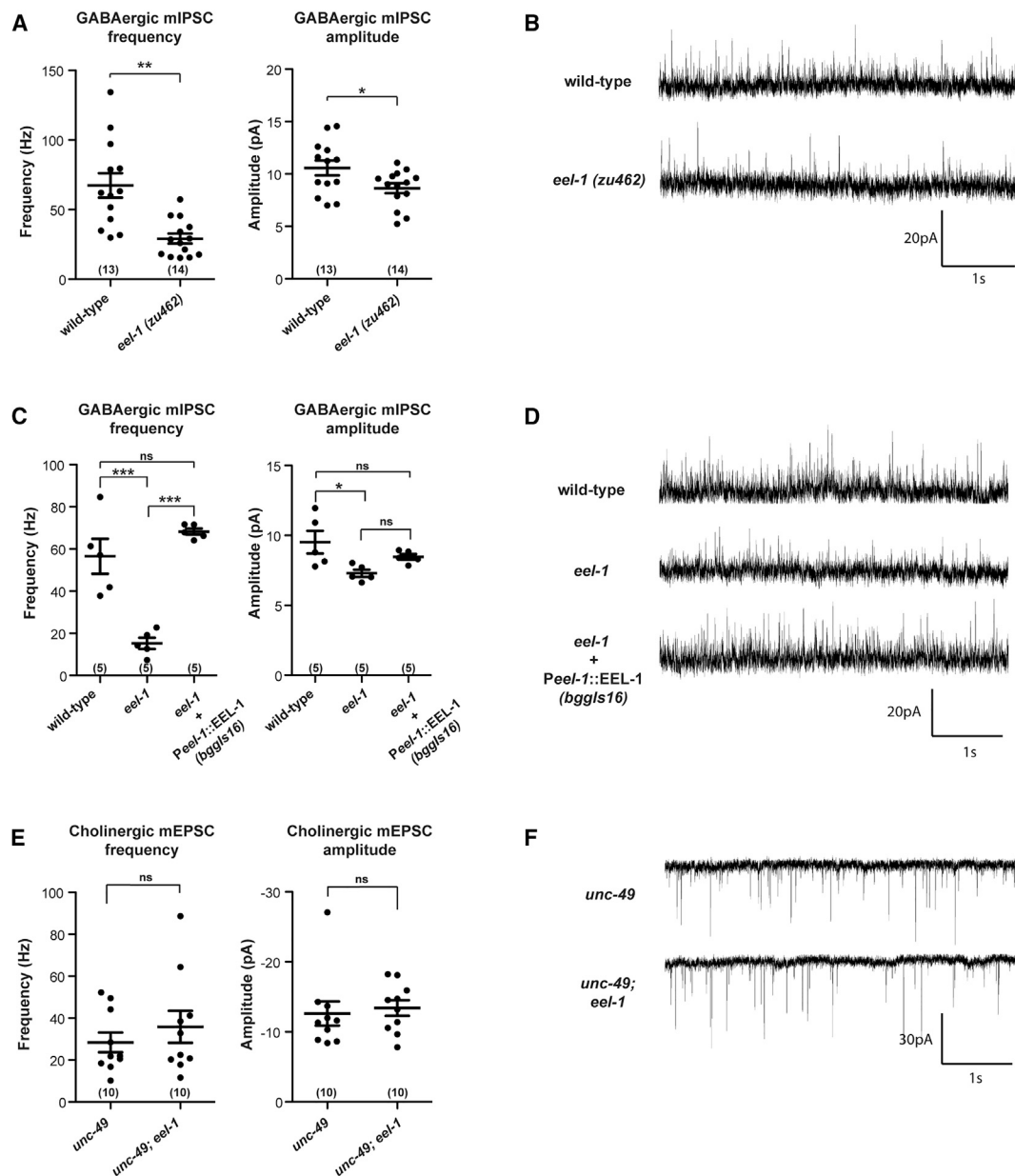


**Figure 3. EEL-1 Is Required for GABAergic Transmission at the NMJ**

(A) GABAergic mIPSC frequency is reduced in *eel-1* (*zu462*) mutants.

(B) Representative GABAergic traces for the indicated genotypes.

(C) The integrated transgenic line *bggls16* (*Peel-1::EEL-1*) rescues GABAergic mIPSC frequency defects in *eel-1* mutants.

(D) Representative GABAergic traces for the indicated genotypes.

(E) Cholinergic mEPSC frequency and amplitude are unchanged in *eel-1* mutants.

(F) Representative cholinergic traces for the indicated genotypes.

\* $p < 0.05$ , \*\* $p < 0.01$ , \*\*\* $p < 0.001$ .

### ***eel-1* Mutants Have Impaired Locomotion and Heightened Sensitivity to Electroshock**

Our pharmacological and electrophysiological results showed that *eel-1* mutants have impaired GABAergic motor neuron function. To test how this affects animal behavior, we analyzed locomotion. Consistent with partially impaired GABAergic transmission, *eel-1* (*lf*) animals displayed a mild uncoordinated

phenotype. We assessed locomotion quantitatively by testing reverse locomotion following harsh head touch and analyzing forward locomotion during spontaneous exploration using Multi-Worm Tracker (MWT).

Following harsh touch, *eel-1* mutants reversed as frequently as wild-type animals (Figure S4), but the distance they reversed was significantly reduced (Figure 5A). Reverse locomotion

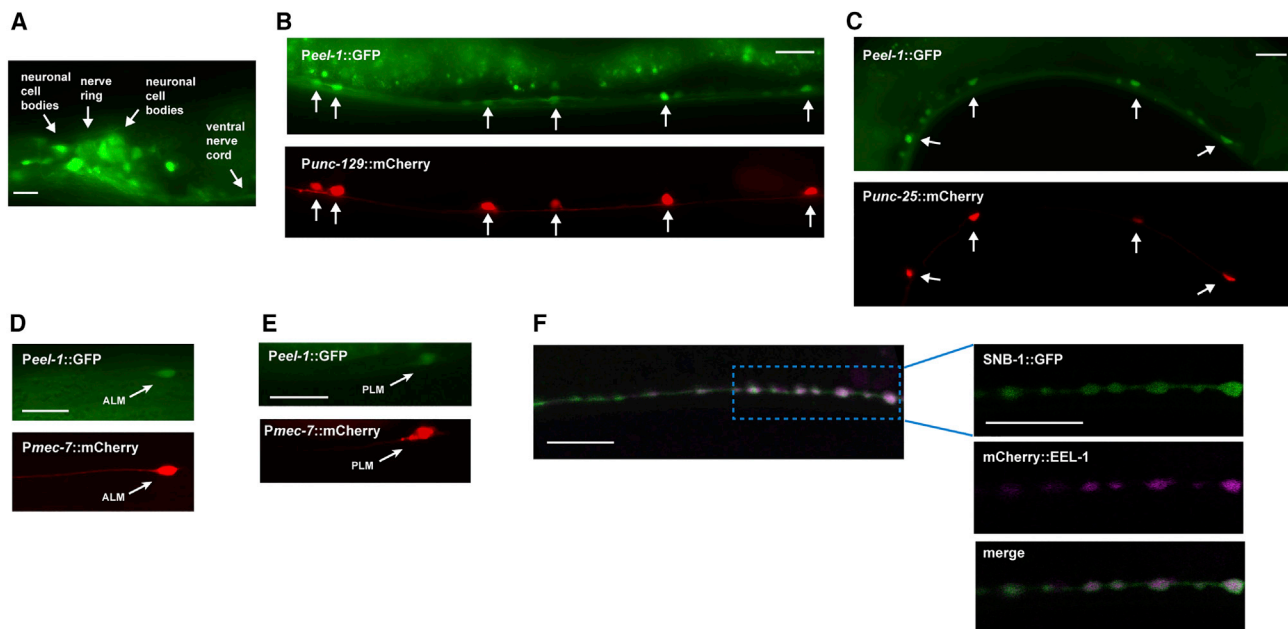


**Figure 4. EEL-1 Is Expressed in the Nervous System and Present at GABAergic Presynaptic Terminals**

Transgenic animals expressing *Peel-1::GFP* were analyzed using epifluorescent microscopy.

(A) Shown are representative images of neurons in the head, the nerve ring, and the ventral nerve cord.

(B) Cholinergic motor neurons (arrows) coexpressing *Peel-1::GFP* and *Punc-129::mCherry* (cholinergic marker).

(C) GABAergic motor neurons (arrows) coexpressing *Peel-1::GFP* and *Punc-25::mCherry* (GABAergic marker).

(D) ALM mechanosensory neuron (arrow) coexpressing *Peel-1::GFP* and *Pmec-7::mCherry* (ALM marker).

(E) PLM mechanosensory neuron (arrow) coexpressing *Peel-1::GFP* and *Pmec-7::mCherry* (PLM marker).

(F) GABAergic presynaptic terminals in the dorsal cord coexpressing *SNB-1::GFP* (*juls1*, green) and *mCherry::EEL-1* (magenta). Left: a merged confocal image of a multi-slice z projection. Right: a higher magnification of a single confocal slice.

Scale bars, 10  $\mu$ m.

defects were rescued by transgenic EEL-1 expressed with a native *eel-1* or pan-neuronal promoter (Figure 5A). *eel-1* mutants did not show the “shrinker” phenotype that occurs when GABAergic transmission is fully impaired, as in *unc-25* mutants (data not shown).

The forward speed of *eel-1* mutants was also significantly slower than in wild-type animals (Figure 5B). This defect was rescued by the *bggls16* transgene that expresses EEL-1 using the native promoter (Figure 5C). These results show that EEL-1 is required for both forward and reverse locomotion. This is consistent with prior studies showing that GABAergic transmission regulates forward and reverse locomotion and that partially impaired GABAergic transmission results in moderate locomotion defects (Petrasch et al., 2013).

Another behavior that is sensitive to E/I balance in the worm motor circuit is electroshock-induced paralysis (Risley et al., 2016). Electroshock involves the application of voltage to animals suspended in saline buffer and results in body convulsions and paralysis. Consistent with prior work, *unc-25/GAD* mutants (which lack inhibitory GABAergic transmission) displayed increased electroshock sensitivity with longer time to recovery (Figure 5D; Risley et al., 2016). Recovery time was also increased in *eel-1* mutants and rescued by *bggls16* (Figure 5D). Pretreatment of *eel-1* animals with retigabine (RTG), a potassium channel agonist and anticonvulsant, rescued electroshock susceptibility

(Figure 5E). RTG most likely activates a potassium channel(s) that alleviates hyperexcitation of muscles, which results from reduced GABAergic transmission in *eel-1* mutants. These behavioral results provide further evidence that EEL-1 regulates GABAergic transmission and is needed for E/I balance.

### EEL-1 and Synapse Formation

One possible explanation for reduced GABAergic presynaptic transmission could be impaired synapse formation in *eel-1* (lf) mutants. To address this, we examined the formation of presynaptic terminals at NMJs made by cholinergic and GABAergic motor neurons.

The motor neuron cell bodies are on the ventral side of *C. elegans* and extend axons that innervate dorsal muscles (Figures 6A and 6C). Each cholinergic motor neuron extends a single axon, and individual GABAergic axons bifurcate. Both types of motor axons form evenly distributed presynaptic connections along dorsal muscles (White et al., 1976).

NMJ formation was evaluated using transgenes that express *SNB-1::GFP* in cholinergic or GABAergic motor neurons. In wild-type animals, *SNB-1* forms puncta at cholinergic and GABAergic presynaptic terminals that are evenly distributed along the dorsal cord (Figures 6A and 6C). Cholinergic NMJs of *eel-1* mutants had mild *SNB-1* defects with small gaps and aggregated puncta (Figure 6A). Quantitation showed reduced

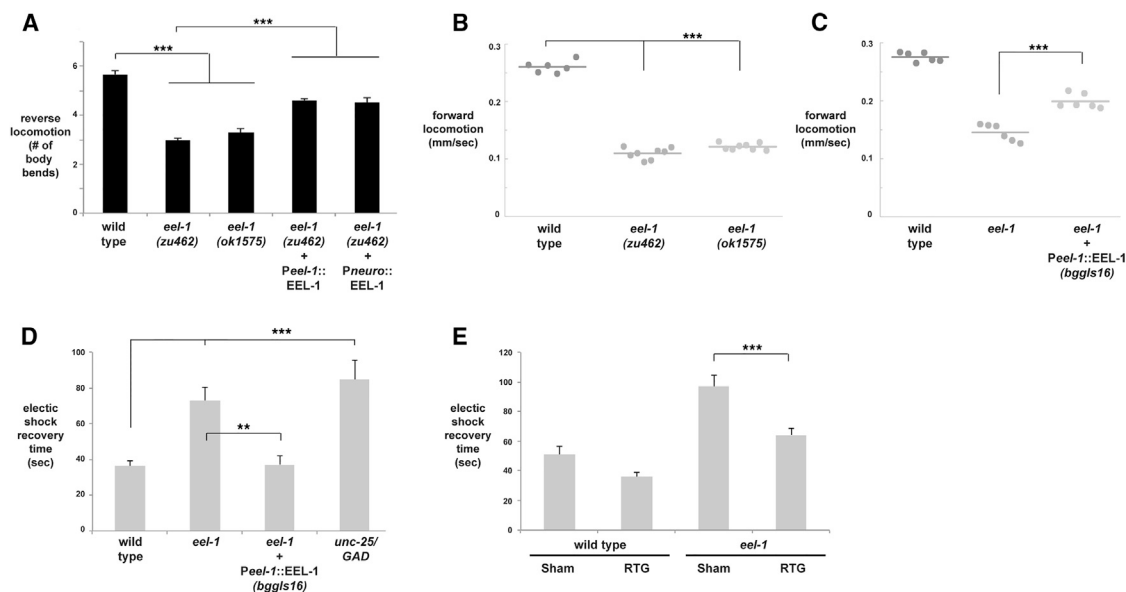


**Figure 5. Locomotion and Electroshock Response Are Impaired in *eel-1* Mutants**

(A) Quantitation of reverse locomotion following harsh head touch for the indicated genotypes.

(B) MWT analysis indicates forward locomotion is impaired in *eel-1* mutants.

(C) Transgenic expression of EEL-1, *bggls16* (*Peel-1::EEL-1*), rescues forward locomotion defects in *eel-1* mutants.

(D) Quantitation of time to recovery following electroshock-induced paralysis. Recovery from electroshock is impaired in *eel-1* mutants and rescued by the transgene *bggls16*.

(E) Treatment of *eel-1* mutants with RTG suppresses defects in recovery from electroshock.

Significance was determined using unpaired Student's t test. Error bars represent SEM. \*\* $p < 0.01$ , \*\*\* $p < 0.001$ .

numbers of puncta in *eel-1* mutants (Figure 6B). In contrast, GABAergic motor neurons of *eel-1* animals had normal organization of SNB-1 puncta (Figures 6C and 6D). Because cholinergic transmission is normal in *eel-1* mutants (Figures 3E and 3F), these mild defects in cholinergic NMJ organization do not impair synaptic transmission. Normal organization of GABAergic SNB-1 puncta suggests that defects in GABAergic transmission in *eel-1* mutants are not caused by defective synapse formation or impaired axon guidance. Normal GABAergic axon guidance was confirmed for *eel-1* mutants using the *juls76* transgene, which expresses soluble GFP in GABAergic neurons (data not shown). Previous studies showed that defects in active zone formation also impair SNB-1 organization in motor neurons, further suggesting that GABAergic synapse formation is largely normal in *eel-1* mutants (Zhen and Jin, 1999).

Disorganized cholinergic presynaptic terminals in *eel-1* mutants are reminiscent of defects that occur with loss of function in *rpm-1*, an intracellular signaling protein that regulates synapse formation (Grill et al., 2016; Zhen et al., 2000). Therefore, we tested the genetic relationship between *eel-1* and *rpm-1*. Consistent with prior studies, cholinergic motor neurons in *rpm-1* mutants had aggregated SNB-1 puncta and gaps lacking puncta (Figure 6A; Nakata et al., 2005). Quantitation showed that *rpm-1* mutants have a more severe phenotype than *eel-1* mutants, which is not increased in *rpm-1; eel-1* double mutants (Figures 6A and 6B). These results suggest that *eel-1* and *rpm-1* function in the same genetic pathway to regulate presynaptic organization of cholinergic NMJs.

Because EEL-1 affects cholinergic synapse formation and functions in the same pathway as RPM-1, we examined GABAergic synapse formation more thoroughly using a sensitizing genetic background. Previous studies showed that FSN-1 mediates a portion of RPM-1 function, and *fsn-1* (*lf*) mutants have milder synapse formation defects than *rpm-1* (*lf*) mutants (Figures 6C and 6D; Grill et al., 2007; Liao et al., 2004). As a result, *fsn-1* (*lf*) can act as a sensitizing background to reveal enhancer effects on GABAergic synapse formation. We observed that *fsn-1; eel-1* double mutants had more severe defects in SNB-1 organization than *fsn-1* single mutants (Figure 6D). These results show that *fsn-1* and *eel-1* function in parallel genetic pathways to regulate GABAergic synapse formation.

Next, we tested *rpm-1; eel-1* double mutants for defects in GABAergic presynaptic organization. Double mutants did not have increased severity of defects compared with *rpm-1* single mutants (Figures 6C and 6D). Thus, *eel-1* and *rpm-1* function in the same genetic pathway to regulate GABAergic presynaptic organization. These results suggest that EEL-1 regulates cholinergic and GABAergic synapse formation by functioning in the RPM-1 pathway and in parallel to FSN-1.

### EEL-1 Regulates Axon Termination and Axon Branch Formation

Aside from its role in synapse formation, RPM-1 is also an important regulator of axon termination (Schaefer et al., 2000). Given that *eel-1* and *rpm-1* function in the same pathway to regulate

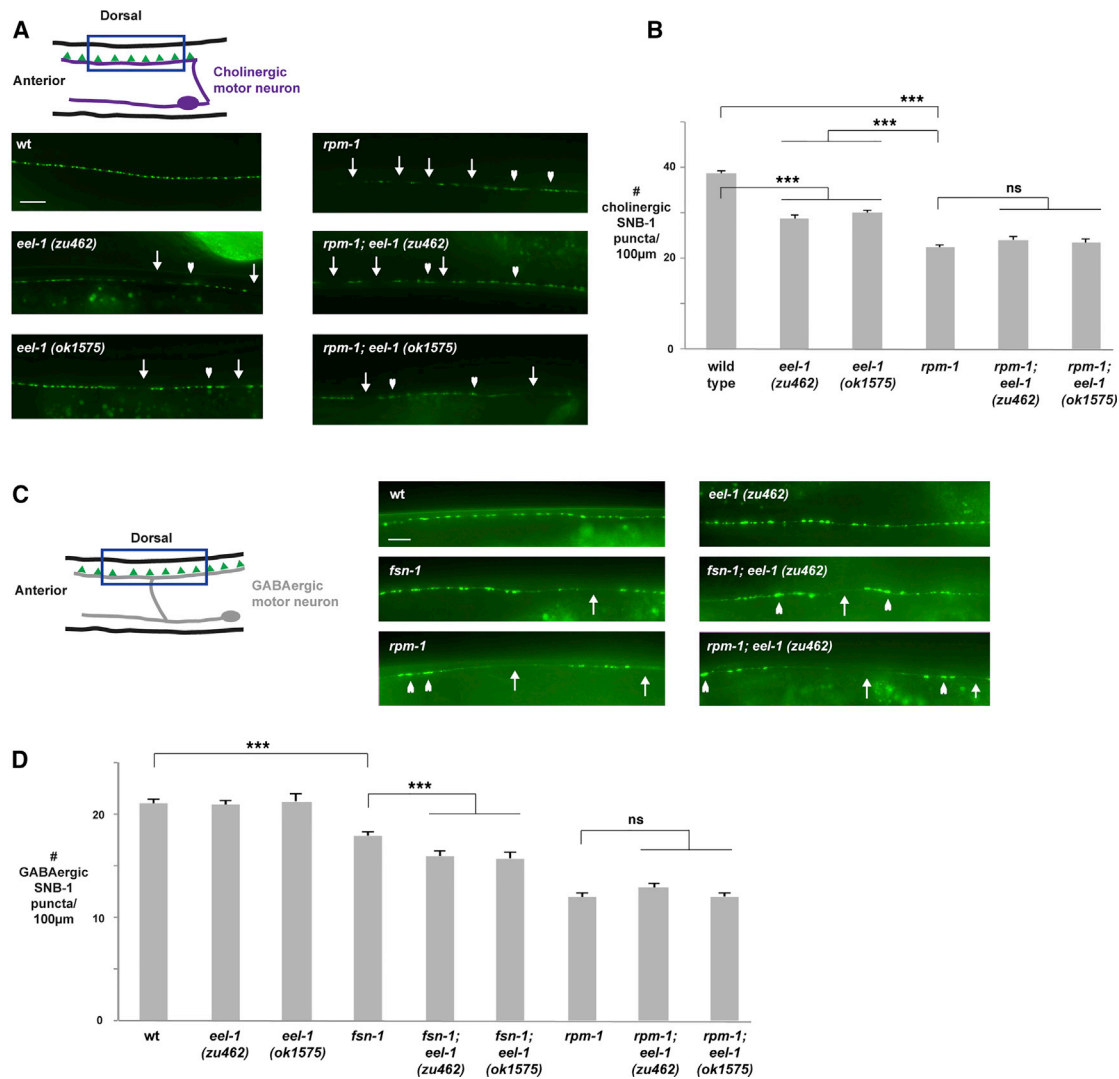


**Figure 6. Motor Neuron Synapse Formation Is Largely Normal in *eel-1* Mutants but Enhanced Synapse Formation Defects Are Present in *eel-1; fsn-1* Double Mutants**

(A) Schematic of a cholinergic motor neuron (purple) innervating dorsal muscles. Presynaptic terminals are shown in green. The blue box highlights the region of the dorsal cord that was visualized using the transgene *nuls152* (*Punc-129::SNB-1::GFP*) for the indicated genotypes. Highlighted are regions lacking SNB-1 puncta (arrows) and abnormal SNB-1 aggregation (arrowheads).

(B) Quantitation of SNB-1 puncta in cholinergic motor neurons for the indicated genotypes.

(C) Schematic of a GABAergic motor neuron (purple) innervating dorsal muscles. Presynaptic terminals are shown in green. The blue box highlights the region of the dorsal cord visualized using the transgene *juls1* (*Punc-25::SNB-1::GFP*) for the indicated genotypes.

(D) Quantitation of SNB-1 puncta in GABAergic motor neurons for the indicated genotypes.

Significance was determined using unpaired Student's *t* test. Error bars represent SEM. \*\*\**p* < 0.001. Scale bar, 10 µm.

synapse formation, we tested whether EEL-1 regulates axon termination.

Axon termination can be rapidly evaluated in the cholinergic SAB neurons that innervate head muscles using *jsIs42*, a transgene with cell-specific expression of SNB-1::GFP (Figure S5A). In wild-type animals, SNB-1 forms puncta at presynaptic terminals along SAB axons and at axon termination sites (Figure S5A). Axon termination defects occurred at moderate frequency in *eel-1* mutants (Figures S5A and S5B). Small ectopic axon branches, often referred to as sprouts, were also observed in

*eel-1* mutants (Figures S5A and S5B). In some instances, axon termination and ectopic branch defects occurred in the same SAB axon (Figure S5A).

Consistent with prior work (Schaefer et al., 2000), *rpm-1* (lf) mutants displayed axon termination and ectopic axon branch defects that were similar to, but more frequent than, *eel-1* mutants (Figures S5A and S5B). The frequency of termination and branch defects did not increase in *rpm-1; eel-1* double mutants (Figure S5B). Similar results were observed for the anterior lateral microtubule (ALM) and posterior lateral microtubule (PLM)

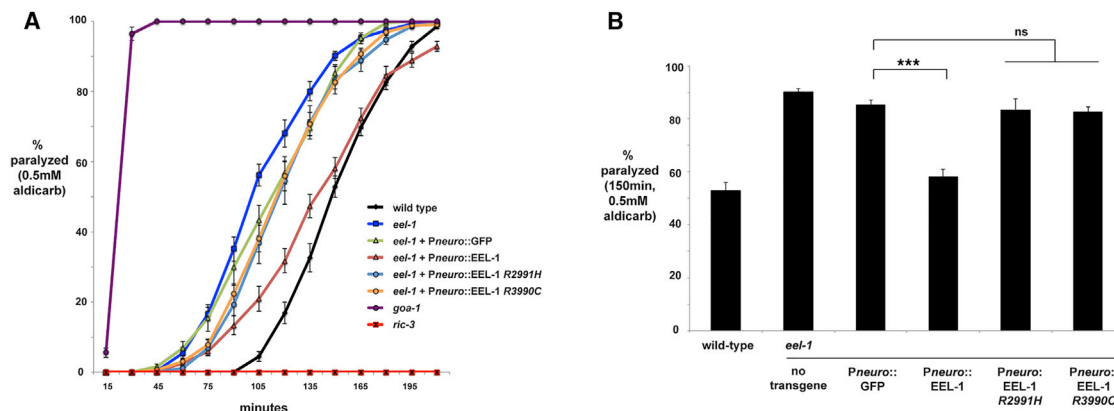


**Figure 7. Conserved, Disorder-Associated Mutations Impair EEL-1**

Wild-type EEL-1 or EEL-1 carrying point mutations associated with intellectual disability (EEL-1 R2991H or R3990C) were tested for transgenic rescue of aldicarb hypersensitivity in *eel-1* mutants.

(A) Aldicarb time course for the indicated genotypes.

(B) Aldicarb paralysis at the 150-min time point for the indicated genotypes. \*\*\* $p < 0.001$ .

mechanosensory neurons (Figure S6), which is consistent with *eel-1* expression in these cells (Figures 4D and 4E). These results using two different types of neurons indicate that *eel-1* and *rpm-1* function in the same genetic pathway to promote axon termination and inhibit ectopic axon branching.

Next we wanted to test whether *eel-1* functions cell-autonomously in SAB neurons to regulate axon development. As shown in Figure S5C, transgenic expression of EEL-1 using an SAB promoter significantly rescued ectopic axon branch defects and axon termination defects. In contrast, rescue did not occur with the negative control mCherry (Figure S5C). Thus, *eel-1* functions cell-autonomously in SAB neurons to regulate axon termination and branch formation.

In mammals, Huwe1 ubiquitinates and inhibits N-Myc to regulate neuronal progenitor proliferation (Zhao et al., 2008, 2009). To test whether EEL-1 regulates axon termination through a similar mechanism, we generated double mutants of *eel-1* with the single worm homolog for the Myc and Mondo transcription factors called Myc/Mondo-like 1 (MML-1). Because MML-1 functions in a complex with MXL-2, the ortholog of mammalian Mxl, we also tested *eel-1*; *mxl-2* double mutants. Our analysis relied on previously described null alleles of *mml-1* and *mxl-2*. Axon termination defects and ectopic branch defects in *eel-1* mutants were not suppressed in *eel-1*; *mml-1* or *eel-1*; *mxl-2* double mutants (Figure S5D). Because suppression would be expected if MML-1/Myc were ubiquitinated and inhibited by EEL-1, these results suggest that EEL-1 is unlikely to regulate axon development via this mechanism.

### Mutations Associated with Intellectual Disability Result in Loss of *eel-1* Function

At present, seven different missense mutations in *HUWE1* are associated with intellectual disability, and several mutations affect residues conserved in *C. elegans* EEL-1 (Friez et al., 2016; Froyen et al., 2008). Two of these mutations are shown in Figure 1A. The functional consequences of these mutations remain unknown. We tested whether EEL-1 containing disorder-

associated mutations can rescue defects caused by *eel-1* (lf). Unlike wild-type EEL-1, transgenic EEL-1 R2991H (which corresponds to HUWE1 R2981H) failed to rescue axon termination and axon branch defects in *eel-1* mutants (Figure S5C). This suggests that EEL-1 R2991H is a loss-of-function mutation.

It is possible that disorder-associated mutations might impair EEL-1 in some contexts but not others. Therefore, we tested whether transgenic EEL-1 containing disorder-associated mutations can rescue the aldicarb hypersensitivity of *eel-1* mutants. Although transgenic expression of wild-type EEL-1 robustly rescued aldicarb hypersensitivity, rescue was not observed with EEL-1-containing, disorder-associated mutations R2991H (which corresponds to HUWE1 R2981H) or R3990C (which corresponds to HUWE1 R4187C) (Figure 7). Thus, the results from two different in vivo assays indicate that mutations in *HUWE1* associated with intellectual disability result in loss of *eel-1* function.

### DISCUSSION

EEL-1 is a HECT family ubiquitin ligase orthologous to mammalian HUWE1. Copy number increases and missense mutations in *HUWE1* are associated with intellectual disability. Previous work showed that Huwe1 regulates neurogenesis and migration of neural progenitors.

Our findings with genetic, pharmacological, and electrophysiological approaches now indicate that EEL-1 regulates presynaptic transmission in GABAergic motor neurons. Furthermore, our results show that EEL-1 is required to obtain E/I balance in the worm motor circuit. *eel-1* mutants have defective locomotion and increased sensitivity to electroshock, consistent with impaired GABAergic transmission and E/I imbalance. We also observed that mutations in *HUWE1* associated with intellectual disability result in loss of EEL-1 function in the context of GABAergic transmission. These findings expand our understanding of the molecular mechanisms required to establish E/I balance in a simple model circuit and could have important implications for the link between HUWE1 and intellectual disability.

### EEL-1 Regulates Inhibitory, GABAergic Presynaptic Transmission

We used the acetylcholinesterase inhibitor aldicarb to pharmacologically assess motor circuit function in *eel-1* mutants. *eel-1* (*lf*) mutants are hypersensitive to aldicarb, and transgenic animals overexpressing EEL-1 display the opposing phenotype—aldicarb resistance (Figures 1 and 2). Thus, decreasing or increasing EEL-1 activity alters motor circuit function. Transgenic rescue and overexpression experiments show that EEL-1 functions cell-autonomously in GABAergic motor neurons to affect aldicarb sensitivity. Although our results suggest that the aldicarb hypersensitivity of *eel-1* (*lf*) mutants is unlikely to stem from defects in synapse or axon development of GABAergic motor neurons, a more thorough analysis of GABAergic NMJs will be needed to entirely rule this out. Nonetheless, our results indicate that reduced GABAergic transmission in *eel-1* mutants leads to E/I imbalance in the motor circuit and aldicarb hypersensitivity.

We confirmed this interpretation of aldicarb results using electrophysiology. *eel-1* (*lf*) mutants have a reduced frequency of GABAergic mIPSCs (Figure 3A). The amplitude of GABAergic mIPSCs was also mildly but significantly reduced in *eel-1* mutants. These results indicate that EEL-1 predominantly affects presynaptic GABAergic transmission. In contrast, both the frequency and amplitude of cholinergic mEPSCs are unchanged in *eel-1* mutants, indicating that cholinergic transmission is unaffected by *eel-1* (*lf*). These pharmacological and electrophysiological data allow us to conclude that reduced inhibitory GABAergic input to muscles in *eel-1* mutants leads to a net increase in E/I ratio from the motor circuit. Impaired GABAergic transmission in *eel-1* (*lf*) mutants is likely to explain why these animals have behavioral abnormalities, including reduced locomotion and increased electroshock sensitivity.

Although EEL-1 functions in GABAergic motor neurons to regulate aldicarb hypersensitivity and presynaptic transmission, EEL-1 does not function exclusively in these neurons. EEL-1 is expressed in both GABAergic and cholinergic motor neurons (Figure 4). This suggests that EEL-1 is required to obtain motor circuit E/I balance rather than being required exclusively for GABAergic transmission. Broad nervous system expression also suggests that EEL-1 might regulate neurotransmission in other neurons.

EEL-1 colocalizes with SNB-1, suggesting that EEL-1 could regulate GABAergic transmission locally (Figure 4F). Consistent with this, Huwe1 associates with the synaptic proteasome in cultured neurons (Tai et al., 2010). Further evidence that EEL-1 ubiquitin ligase activity might regulate synaptic transmission stems from two observations: both *eel-1* deletion alleles result in loss of the HECT ubiquitin ligase domain (Figure 1A), and a disorder-associated point mutation in the HECT domain, *R3990C*, impairs EEL-1 function (Figure 7). However, ubiquitin ligase-independent mechanisms cannot be ruled out because a mutation outside of the HECT domain (*R2991H*) also impairs EEL-1 function.

At present, little is known about ubiquitin ligases that regulate presynaptic transmission in vivo. In mice, Scrapper degrades RAB3 interacting molecule (RIM) to inhibit presynaptic transmission (Yao et al., 2007). Parkin and the anaphase promoting com-

plex (APC) regulate presynaptic transmission at the fly and worm NMJ (Kowalski et al., 2014; van Roessel et al., 2004; Vincent et al., 2012). Notably, Scrapper, Parkin, and the APC are RING family ubiquitin ligases. Our findings now show that a HECT ubiquitin ligase, EEL-1, preferentially regulates GABAergic transmission.

### EEL-1 and Synaptic Transmission: Implications for HUWE1 and Intellectual Disability

The worm motor circuit requires E/I balance for proper function, which makes this model circuit valuable for studying the molecular and cellular mechanisms of neurodevelopmental disorders (Bessa et al., 2013). Our results indicate that EEL-1 is required for GABAergic presynaptic transmission and E/I balance in the motor circuit. Like the worm motor circuit, GABA is inhibitory in the mammalian brain. The obvious caveats of our simple system aside, if HUWE1 is a conserved regulator of GABAergic transmission, then increased or reduced HUWE1 function might affect E/I balance in the brain. This could have important implications for *HUWE1* and intellectual disability because E/I imbalances occur in many neurodevelopmental disorders (Gatto and Broadie, 2010; Rubenstein and Merzenich, 2003).

Increased copies of *HUWE1* are associated with intellectual disability, and missense mutations in *HUWE1* are associated with intellectual disability as part of Juberg-Marsidi-Brooks syndrome. An explanation for how differing *HUWE1* genetic changes lead to intellectual disability remains absent. Using in vivo neuronal assays, we have shown that two mutations associated with intellectual disability impair *eel-1* function (Figure 7). The mutated residues are identical in EEL-1 and HUWE1, suggesting that they are likely to result in loss of HUWE1 function. Nonetheless, these mutations are presumably hypomorphic in some contexts (for example, early neurogenesis) because *Huwe1* knockout is lethal (Zhao et al., 2009). Overexpression of EEL-1 in GABAergic motor neurons results in altered motor circuit function and resistance to aldicarb. Thus, copy number increases in *HUWE1* could potentially affect GABAergic transmission. If increased and reduced *HUWE1* function are associated with intellectual disability, *HUWE1* would join *SHANK3* and *MECP2* as genes with both gain- and loss-of-function changes associated with intellectual disability (Zoghbi and Bear, 2012).

Our previous work showed that impaired GABAergic transmission caused by *unc-25/GAD* (*lf*) results in E/I imbalance in the motor circuit and increased sensitivity to electroshock (Risley et al., 2016). *eel-1* (*lf*) mutants also have increased electroshock sensitivity, consistent with reduced GABAergic transmission (Figure 5D). This defect is suppressed by the anticonvulsant RTG, an agonist for KCNQ2/3 voltage-gated potassium channels in mice and flies (Barrese et al., 2010). Although it is unclear how RTG rescues *eel-1* mutants, one possibility is that RTG relieves hyperexcitation in *eel-1* mutants by stimulating potassium channels. Given that electroshock is often used to study seizure in different systems and keeping in mind the limitations of our worm electroshock assay, it is noteworthy that subsets of individuals with genetic changes in *HUWE1* experience seizures (Froyen et al., 2008, 2012).

### ***eel-1* and *rpm-1* Function in the Same Pathway to Regulate Neuronal Development**

EEL-1 and Huwe1 are single-subunit ubiquitin ligases of the HECT family. The HECT family includes Ube3a, Nedd4, and Smurf, which have important roles in neuronal development (Ambrozkiewicz and Kawabe, 2015; Yamada et al., 2013). Previous work showed that EEL-1 and Huwe1 regulate neural progenitor proliferation and migration (de Groot et al., 2014; Forget et al., 2014; Zhao et al., 2009). We have explored the role of EEL-1 in later developmental events, such as synapse formation and axon termination.

Axon termination defects in SAB neurons and mechanosensory neurons were the most prevalent developmental defects we observed in *eel-1* (lf) mutants (Figures S5 and S6). Small ectopic axon branches, referred to as sprouts, were also observed in the SAB neurons of *eel-1* (lf) mutants. Previous work showed that transgenic overexpression of Huwe1 results in ectopic axon branching in flies (Vandewalle et al., 2013). Our findings and this prior work indicate that decreasing or increasing EEL-1/Huwe1 function can affect axon termination and branching.

We examined presynaptic organization in cholinergic and GABAergic motor neurons of *eel-1* (lf) mutants. As mentioned earlier, GABAergic presynaptic organization was normal in *eel-1* mutants (Figures 6C and 6D). We observed mild defects in cholinergic motor neurons, which did not impair cholinergic transmission. Thus, EEL-1 figures more prominently in GABAergic transmission and has a minor role in presynaptic organization in cholinergic motor neurons. Although our results indicate that motor neuron synapse formation is largely normal in *eel-1* mutants, they do not rule out the possibility subtle defects in presynaptic terminals could affect GABAergic transmission.

Axon termination defects and cholinergic presynaptic organization defects in *eel-1* mutants were similar, but milder, than what occurs in *rpm-1* mutants. Therefore, we explored the genetic relationship between *eel-1* and *rpm-1* in synapse and axon development. Previous work established RPM-1 and orthologous Pam/Highwire/RPM-1 (PHR) proteins as regulators of synapse and axon development (Grill et al., 2016). RPM-1 is an intracellular signaling hub that regulates several downstream pathways (Baker et al., 2014; Grill et al., 2007, 2012; Nakata et al., 2005; Tulgren et al., 2014). Our analysis indicates that *fsn-1*, an F box protein that mediates a portion of RPM-1 signaling, functions in a parallel pathway with *eel-1* to regulate GABAergic synapse formation and axon termination (Figures 6C and 6D; Figure S6). Like other *fsn-1* enhancers, *eel-1* functions in the same genetic pathway as *rpm-1*. These genetic results are consistent with EEL-1 and RPM-1 localizing to GABAergic presynaptic terminals (Figure 4F; Zhen et al., 2000).

Work using non-neuronal cells showed that the RPM-1 ortholog Pam/MYCBP2 can function in a ubiquitin ligase complex with Huwe1 (Yin et al., 2010). Our genetic results suggest that RPM-1 could function in one complex with EEL-1 and in a different complex with FSN-1. Prior evidence indicates that RPM-1 can function through two mechanisms, RPM-1/FSN-1 ubiquitin ligase activity and RPM-1 recruitment of the PPM-2 phosphatase, to restrict the DLK-1 mitogen activated protein kinase

kinase kinase (MAP3K) (Baker et al., 2014; Nakata et al., 2005). Thus, RPM-1 might utilize FSN-1 and EEL-1 as different mechanisms to regulate DLK-1 or other molecules in the DLK-1/PMK-3 p38 mitogen-activated protein kinase (MAPK) pathway.

Another potential link between EEL-1 and RPM-1 is  $\beta$ -catenin signaling. EEL-1 regulates neuroblast migration by inhibiting the Wnt effector protein Dishevelled, which regulates  $\beta$ -catenin (de Groot et al., 2014). RPM-1 regulates axon termination and synapse formation by binding to the Nesprin ANC-1 and regulating  $\beta$ -catenin signaling (Tulgren et al., 2014). Therefore, RPM-1 and EEL-1 might function in the same genetic pathway because they both affect  $\beta$ -catenin signaling.

Genetic and molecular links between RPM-1 signaling and neurodevelopmental disorders have begun to emerge. For example, Pam regulates the tuberous sclerosis complex (TSC), which is linked to tuberous sclerosis and autism (Han et al., 2012; Murthy et al., 2004). Microduplications and microdeletions that include *Fbxo45*, the ortholog of FSN-1, are associated with neurodevelopmental disorders (Grill et al., 2016). Our findings now provide in vivo genetic evidence from a model system linking the RPM-1 signaling network to *eel-1*, a gene associated with intellectual disability.

### **Conclusions**

Our results with a simple model circuit indicate that EEL-1 regulates presynaptic GABAergic transmission. This EEL-1 function is required for proper locomotion, affects sensitivity to electroshock, and provides important insight into the molecular mechanisms required to establish E/I balance. Our findings could also have important implications for the link between EEL-1 and intellectual disability, which is heightened by our observation that mutations associated with intellectual disability lead to loss of EEL-1 function in neurons in vivo. Although we have learned much about the electrophysiological and cellular mechanisms by which EEL-1 regulates GABAergic transmission, an intriguing and challenging future goal will be understanding the molecular mechanisms by which EEL-1 regulates GABAergic transmission.

### **EXPERIMENTAL PROCEDURES**

Further details and expanded methods can be found in the [Supplemental Experimental Procedures](#).

#### **Strains and Genetics**

The *C. elegans* N2 isolate was propagated and maintained using standard procedures. The alleles used included *eel-1* (*zu462*), *eel-1* (*ok1575*), *rpm-1* (*ju44*), *rpm-1* (*ok364*), *fsn-1* (*gk429*), *goa-1* (*n363*), *ric-3* (*md158*), *unc-4* (*e120*), *mml-1* (*ok849*), *mxl-2* (*tm1516*), and *unc-49* (*e407*). The integrated transgenic strains used included *jsls42* [ $P_{unc-4}$ SNB-1::GFP], *nuls152* [ $P_{unc-129}$ SNB-1::GFP], *juls1* [ $P_{unc-25}$ SNB-1::GFP], *muls32* [ $P_{mec-7}$ GFP], *juls76* [ $P_{unc-25}$ GFP], and *bggls16* [ $P_{eel-1}$ ,EEL-1].

We sequenced to confirm the nature of the lesions in *ok1575* and *zu462*. *ok1575* is a 1,637-bp deletion that removes intronic and exonic sequences. Failed splicing in *ok1575* is likely to create a premature stop, resulting in loss of more than 50% of the EEL-1 sequence, including the HECT ubiquitin ligase domain (Figure 1A). *zu462* is an inverted duplication that results in a large deletion and insertion of 5,884 bp. *zu462* disrupts the *eel-1* reading frame, leads to 36 amino acids of non-sense sequence and a stop codon, and results in a truncated protein lacking a HECT domain (Figure 1A).

### Transgenics

Transgenic animals were generated using standard microinjection procedures. Extrachromosomal transgenic arrays were constructed by injecting animals with the plasmid or PCR product of interest,  $P_{\text{ttx-3}}$ RFP (50 ng/ $\mu\text{L}$ ) or  $P_{\text{myo-2}}$ mCherry (1 ng/ $\mu\text{L}$ ) as coinjection marker, and pBluescript (25–90 ng/ $\mu\text{L}$ ) to normalize injections to 100 ng/ $\mu\text{L}$  total DNA. For *eel-1* promoter expression, shown in Figure 4, *pha-1(e2123)* was used as a temperature-sensitive positive selection marker. The precise composition of injection mixtures and genotypes of animals used in this study are annotated in Table S1. The transgenic line *bggIs16* [ $P_{\text{eel-1}}$ EEL-1] was generated by UV/4,5',8-trimethylpsoralen (TMP) integration of *bggEx117*. *bggIs16* was outcrossed seven times to N2 worms and mated to *eel-1* (*zu462*) for rescue experiments. *bggEx117* was generated by injecting  $P_{\text{eel-1}}$ EEL-1 (pBG-GY550, 75 ng/ $\mu\text{L}$ ),  $P_{\text{myo-2}}$ mCherry (1 ng/ $\mu\text{L}$ ), and pBluescript (25 ng/ $\mu\text{L}$ ).

Transgenic strains used for confocal imaging, shown in Figure 4F and Figure S3, were generated by injecting transgenic animals carrying *juls1* [ $P_{\text{unc-25}}$ SNB-1::GFP] with the following plasmid mixture: pBG-GY656 ( $P_{\text{unc-25}}$ mCherry::EEL-1, 40 ng/ $\mu\text{L}$ ), pBG-GY322 ( $P_{\text{myo-2}}$ mCherry, 1 ng/ $\mu\text{L}$ ), and pBlueScript (60 ng/ $\mu\text{L}$ ). Two independent lines were isolated and analyzed: *bggEx125*; *juls1* and *bggEx126*; *juls1*.

### Aldicarb Assay

Nematode growth media (NGM) plates with aldicarb (Aldicarb-Pestanal, Sigma) and a spot of OP-50 *E. coli* were warmed to room temperature for 3 hr prior to experimentation. Animals (blinded for genotype) were individually touched on the posterior body to assess movement every 15 min. Animals were considered paralyzed when no body or head movement was detected. Initially, for analysis of *eel-1* RNAi and mutants, 1 mM aldicarb was used. To more accurately separate differences in hypersensitivity for different genotypes, subsequent experiments were performed with 0.5 mM aldicarb because this lower concentration enhanced the sensitivity of aldicarb responses. Prior to the aldicarb assays, all strains were grown at 23°C.

### Forward Speed during Exploratory Locomotion

*C. elegans* locomotion was assessed as described previously (Giles et al., 2015). Briefly, *C. elegans* were cultivated at 23°C, and synchronized adults were placed on NGM agar plates without *E. coli* and allowed to spontaneously explore for 5 min. Behavioral recordings of this exploration were taken using an adapted version of MWT. Centroid speed during periods of forward locomotion was measured during the final minute of observation. The average speed of ~30 worms was measured at a time on one plate and considered a single data point; six to nine plates were tested per strain. Some mutants had a significantly smaller body length than the wild-type, which could affect absolute speed. To control for this, speed was standardized to body length. Only absolute speed is presented because similar results were observed when standardized. In-depth details regarding forward locomotion analysis with MWT analysis can be found in the Supplemental Experimental Procedures.

### Electrophysiology

Electrophysiological recordings were performed as described previously (Gao and Zhen, 2011). The intracellular solution contained K-gluconate, 115 mM; KCl, 25 mM;  $\text{CaCl}_2$ , 0.1 mM;  $\text{MgCl}_2$ , 5 mM; 1, 2-bis (o-aminophenoxy) ethane-N, N, N', N'-tetraacetic acid (BAPTA), 1 mM; HEPES, 10 mM;  $\text{Na}_2\text{ATP}$ , 5 mM;  $\text{Na}_2$  guanosine triphosphate (GTP), 0.5 mM; cyclic AMP (cAMP), 0.5 mM; and cyclic GMP (cGMP), 0.5 mM (pH 7.2 with potassium hydroxide [KOH], 320 mOsm). The extracellular solution contained NaCl, 150 mM; KCl, 5 mM;  $\text{CaCl}_2$ , 5 mM;  $\text{MgCl}_2$ , 1 mM; glucose, 10 mM; sucrose, 5 mM; and HEPES, 15 mM (pH 7.3 with NaOH, 330 mOsm). GABAergic mIPSCs were recorded in the presence of 0.5 mM d-tubocurarine in the extracellular solution to block cholinergic receptors while holding the membrane at  $-10$  mV so GABAergic mIPSCs appeared as outward currents (Maro et al., 2015). Cholinergic mEPSCs were recorded in the background of *unc-49* (*e407*), a loss-of-function mutation in the GABA receptor, while holding the membrane at  $-60$  mV. All experiments were performed at room temperature (20°C–22°C).

### Electroshock Assay

The electric shock procedure was performed as described previously (Risley et al., 2016). 1-day-old adult *C. elegans* (approximately 10 animals/electroshock assay) were incubated for 30 min with or without retigabine and subjected to electric shock for three seconds (204 Hz, 47 V). Videos were manually scored to quantify the time needed to recover from electroshock. The Supplemental Experimental Procedures contain further details.

### Analysis of Developmental Phenotypes

Young adult animals were anesthetized using 2% (v/v) 1-phenoxy-2-propanol in M9 buffer. Synchronized young adults were analyzed for cholinergic motor neurons (*nuls152*) and GABAergic motor neurons (*juls1*), whereas non-synchronized young adult animals were analyzed for SAB neurons (*jls42*) and mechanosensory neurons (*muls32*). Analysis with *nuls152*, *juls1*, and *jls42* was done on worms grown at 25°C, and analysis with *muls32* was done on worms grown at 23°C. *jls42* animals were visualized using 63 $\times$  magnification, and *muls32*, *juls1* and *nuls152* animals were visualized using 40 $\times$  magnification oil immersion and an epifluorescence microscope (Leica CRF 5000). Images of anesthetized animals were taken using a charge-coupled device (CCD) camera (Leica DFC345 FX). Image analysis was performed using Leica Application Suite for Advanced Fluorescence (LAS-AF) software. For *nuls152* and *juls1*, images from the dorsal cord were measured using LAS-AF software, and the number of SNB-1::GFP puncta were manually scored using Adobe Photoshop.

### Confocal Microscopy

Animals were paralyzed in 5 mM levamisole. Confocal imaging was done using a Leica TCS SP8 MP confocal microscope system in resonant mode with a 40 $\times$  water immersion lens (HC PL APO 40 $\times$ /1.10 CS2). Images were acquired using the Leica acquisition software with a 2–10 $\times$  zoom factor. ImageJ (version 1.50d) was used to process the images. For presentation of confocal stacks, either a single slice was used, or the maximum intensity projection was used as noted. Further details are available in the Supplemental Experimental Procedures.

### Statistical Analysis

Reported are original Student's *t* test values. In cases where multiple comparisons were performed, Bonferroni corrections were tested, and in all cases statistical significance was maintained. For detailed statistical methods, see the Supplemental Experimental Procedures.

### SUPPLEMENTAL INFORMATION

Supplemental Information includes Supplemental Experimental Procedures, six figures, and one table and can be found with this article online at <http://dx.doi.org/10.1016/j.celrep.2017.04.003>.

### AUTHOR CONTRIBUTIONS

The authors conceived, designed, and performed the experiments as follows. Aldicarb analysis: K.J.O.; developmental analysis: K.J.O., E.D.T., and B.G.; EEL-1 localization and expression studies: A.C.G., R.L.B., and B.G.; automated locomotion analysis: A.C.G.; electrophysiology: B.M. and M.Z.; electroshock analysis: M.G.R. and K.D.S. B.G. wrote the paper with assistance from K.J.O., A.C.G., B.M., and M.G.R.

### ACKNOWLEDGMENTS

We thank Drs. Damon Page, Samuel Young, Jr., and Kirill Martemyanov for helpful discussions and comments on our manuscript. We appreciate the generosity of Dr. Barbara Page for providing *eel-1* (*zu462*), Dr. Mike Nonet for *jls42*, and Dr. Derek Sieburth for *nuls152*. We thank the *C. elegans* Knockout Consortium for generating several alleles, and the *C. elegans* Genetics Center (NIH Office of Research Infrastructure Programs, P40 OD010440) for providing strains. B.G. was supported by grants from the NIH (2R01 NS072129) and the NSF (IOS-1121095).

Received: January 4, 2017  
Revised: March 1, 2017  
Accepted: March 31, 2017  
Published: April 25, 2017

## REFERENCES

- Ambrozkiwicz, M.C., and Kawabe, H. (2015). HECT-type E3 ubiquitin ligases in nerve cell development and synapse physiology. *FEBS Lett.* *589*, 1635–1643.
- Baker, S.T., Opperman, K.J., Tulgren, E.D., Turgeon, S.M., Bienvenut, W., and Grill, B. (2014). RPM-1 uses both ubiquitin ligase and phosphatase-based mechanisms to regulate DLK-1 during neuronal development. *PLoS Genet.* *10*, e1004297.
- Barclay, J.W., Morgan, A., and Burgoyne, R.D. (2012). Neurotransmitter release mechanisms studied in *Caenorhabditis elegans*. *Cell Calcium* *52*, 289–295.
- Barrese, V., Miceli, F., Soldovieri, M.V., Ambrosino, P., Iannotti, F.A., Cilio, M.R., and Tagliatela, M. (2010). Neuronal potassium channel openers in the management of epilepsy: role and potential of retigabine. *Clin. Pharmacol.* *2*, 225–236.
- Bessa, C., Maciel, P., and Rodrigues, A.J. (2013). Using *C. elegans* to decipher the cellular and molecular mechanisms underlying neurodevelopmental disorders. *Mol. Neurobiol.* *48*, 465–489.
- Calixto, A., Chelur, D., Topalidou, I., Chen, X., and Chalfie, M. (2010). Enhanced neuronal RNAi in *C. elegans* using SID-1. *Nat. Methods* *7*, 554–559.
- Cherra, S.J., 3rd, and Jin, Y. (2016). A Two-Immunoglobulin-Domain Transmembrane Protein Mediates an Epidermal-Neuronal Interaction to Maintain Synapse Density. *Neuron* *89*, 325–336.
- de Groot, R.E., Ganji, R.S., Bernatik, O., Lloyd-Lewis, B., Seipel, K., Šedová, K., Zdráhal, Z., Dhople, V.M., Dale, T.C., Korswagen, H.C., and Bryja, V. (2014). Huwe1-mediated ubiquitylation of dishevelled defines a negative feedback loop in the Wnt signaling pathway. *Sci. Signal.* *7*, ra26.
- Forget, A., Bihannic, L., Cigna, S.M., Lefevre, C., Remke, M., Barnat, M., Dodier, S., Shirvani, H., Mercier, A., Mensah, A., et al. (2014). Shh signaling protects Atoh1 from degradation mediated by the E3 ubiquitin ligase Huwe1 in neural precursors. *Dev. Cell* *29*, 649–661.
- Friez, M.J., Brooks, S.S., Stevenson, R.E., Field, M., Basehore, M.J., Adès, L.C., Sebald, C., McGee, S., Saxon, S., Skinner, C., et al. (2016). HUWE1 mutations in Juberg-Marsidi and Brooks syndromes: the results of an X-chromosome exome sequencing study. *BMJ Open* *6*, e009537.
- Froyen, G., Corbett, M., Vandewalle, J., Jarvela, I., Lawrence, O., Meldrum, C., Bauters, M., Govaerts, K., Vandeleur, L., Van Esch, H., et al. (2008). Submicroscopic duplications of the hydroxysteroid dehydrogenase HSD17B10 and the E3 ubiquitin ligase HUWE1 are associated with mental retardation. *Am. J. Hum. Genet.* *82*, 432–443.
- Froyen, G., Belet, S., Martinez, F., Santos-Rebouças, C.B., Declercq, M., Verbeeck, J., Donckers, L., Berland, S., Mayo, S., Rosello, M., et al. (2012). Copy-number gains of HUWE1 due to replication- and recombination-based rearrangements. *Am. J. Hum. Genet.* *91*, 252–264.
- Gao, S., and Zhen, M. (2011). Action potentials drive body wall muscle contractions in *Caenorhabditis elegans*. *Proc. Natl. Acad. Sci. USA* *108*, 2557–2562.
- Gatto, C.L., and Broadie, K. (2010). Genetic controls balancing excitatory and inhibitory synaptogenesis in neurodevelopmental disorder models. *Front. Synaptic Neurosci.* *2*, 4.
- Giles, A.C., Opperman, K.J., Rankin, C.H., and Grill, B. (2015). Developmental Function of the PHR Protein RPM-1 Is Required for Learning in *Caenorhabditis elegans*. *G3 (Bethesda)* *5*, 2745–2757.
- Grill, B., Bienvenut, W.V., Brown, H.M., Ackley, B.D., Quadroni, M., and Jin, Y. (2007). *C. elegans* RPM-1 regulates axon termination and synaptogenesis through the Rab GEF GLO-4 and the Rab GTPase GLO-1. *Neuron* *55*, 587–601.
- Grill, B., Chen, L., Tulgren, E.D., Baker, S.T., Bienvenut, W., Anderson, M., Quadroni, M., Jin, Y., and Garner, C.C. (2012). RAE-1, a novel PHR binding protein, is required for axon termination and synapse formation in *Caenorhabditis elegans*. *J. Neurosci.* *32*, 2628–2636.
- Grill, B., Murphey, R.K., and Borgen, M.A. (2016). The PHR proteins: intracellular signaling hubs in neuronal development and axon degeneration. *Neural Dev.* *11*, 8.
- Han, S., Kim, S., Bahl, S., Li, L., Burande, C.F., Smith, N., James, M., Beauchamp, R.L., Bhide, P., Diantonio, A., and Ramesh, V. (2012). The E3 ubiquitin ligase, protein associated with Myc (Pam) regulates mammalian/mechanistic target of rapamycin complex 1 (mTORC1) signaling in vivo through N- and C-terminal domains. *J. Biol. Chem.* *287*, 30063–30072.
- Isrie, M., Kalscheuer, V.M., Holvoet, M., Fieremans, N., Van Esch, H., and Devriendt, K. (2013). HUWE1 mutation explains phenotypic severity in a case of familial idiopathic intellectual disability. *Eur. J. Med. Genet.* *56*, 379–382.
- Jospin, M., Qi, Y.B., Stawicki, T.M., Boulin, T., Schuske, K.R., Horvitz, H.R., Bessereau, J.L., Jorgensen, E.M., and Jin, Y. (2009). A neuronal acetylcholine receptor regulates the balance of muscle excitation and inhibition in *Caenorhabditis elegans*. *PLoS Biol.* *7*, e1000265.
- Kowalski, J.R., Dube, H., Touroutine, D., Rush, K.M., Goodwin, P.R., Carozza, M., Didier, Z., Francis, M.M., and Juo, P. (2014). The Anaphase-Promoting Complex (APC) ubiquitin ligase regulates GABA transmission at the *C. elegans* neuromuscular junction. *Mol. Cell. Neurosci.* *58*, 62–75.
- Leboucher, G.P., Tsai, Y.C., Yang, M., Shaw, K.C., Zhou, M., Veenstra, T.D., Glickman, M.H., and Weissman, A.M. (2012). Stress-induced phosphorylation and proteasomal degradation of mitofusin 2 facilitates mitochondrial fragmentation and apoptosis. *Mol. Cell* *47*, 547–557.
- Liao, E.H., Hung, W., Abrams, B., and Zhen, M. (2004). An SCF-like ubiquitin ligase complex that controls presynaptic differentiation. *Nature* *430*, 345–350.
- Loria, P.M., Hodgkin, J., and Hobert, O. (2004). A conserved postsynaptic transmembrane protein affecting neuromuscular signaling in *Caenorhabditis elegans*. *J. Neurosci.* *24*, 2191–2201.
- Madrigo, I., Rodríguez-Revenga, L., Armengol, L., González, E., Rodríguez, B., Badenas, C., Sánchez, A., Martínez, F., Guitart, M., Fernández, I., et al. (2007). X-chromosome tiling path array detection of copy number variants in patients with chromosome X-linked mental retardation. *BMC Genomics* *8*, 443.
- Maro, G.S., Gao, S., Olechwier, A.M., Hung, W.L., Liu, M., Özkan, E., Zhen, M., and Shen, K. (2015). MADD-4/Punctin and Neurexin Organize *C. elegans* GABAergic Postsynapses through Neuroigin. *Neuron* *86*, 1420–1432.
- Miller, K.G., Alfonso, A., Nguyen, M., Crowell, J.A., Johnson, C.D., and Rand, J.B. (1996). A genetic selection for *Caenorhabditis elegans* synaptic transmission mutants. *Proc. Natl. Acad. Sci. USA* *93*, 12593–12598.
- Murthy, V., Han, S., Beauchamp, R.L., Smith, N., Haddad, L.A., Ito, N., and Ramesh, V. (2004). Pam and its ortholog highwire interact with and may negatively regulate the TSC1.TSC2 complex. *J. Biol. Chem.* *279*, 1351–1358.
- Nakata, K., Abrams, B., Grill, B., Goncharov, A., Huang, X., Chisholm, A.D., and Jin, Y. (2005). Regulation of a DLK-1 and p38 MAP kinase pathway by the ubiquitin ligase RPM-1 is required for presynaptic development. *Cell* *120*, 407–420.
- Page, B.D., Diède, S.J., Tenlen, J.R., and Ferguson, E.L. (2007). EEL-1, a Hect E3 ubiquitin ligase, controls asymmetry and persistence of the SKN-1 transcription factor in the early *C. elegans* embryo. *Development* *134*, 2303–2314.
- Petrash, H.A., Philbrook, A., Haburcak, M., Barbagallo, B., and Francis, M.M. (2013). ACR-12 ionotropic acetylcholine receptor complexes regulate inhibitory motor neuron activity in *Caenorhabditis elegans*. *J. Neurosci.* *33*, 5524–5532.
- Richmond, J.E., and Jorgensen, E.M. (1999). One GABA and two acetylcholine receptors function at the *C. elegans* neuromuscular junction. *Nat. Neurosci.* *2*, 791–797.
- Risley, M.G., Kelly, S.P., Jia, K., Grill, B., and Dawson-Scully, K. (2016). Modulating Behavior in *C. elegans* Using Electroshock and Antiepileptic Drugs. *PLoS ONE* *11*, e0163786.

- Rubenstein, J.L., and Merzenich, M.M. (2003). Model of autism: increased ratio of excitation/inhibition in key neural systems. *Genes Brain Behav.* *2*, 255–267.
- Schaefer, A.M., Hadwiger, G.D., and Nonet, M.L. (2000). *rpm-1*, a conserved neuronal gene that regulates targeting and synaptogenesis in *C. elegans*. *Neuron* *26*, 345–356.
- Sieburth, D., Ch'ng, Q., Dybbs, M., Tavazoie, M., Kennedy, S., Wang, D., Dupuy, D., Rual, J.F., Hill, D.E., Vidal, M., et al. (2005). Systematic analysis of genes required for synapse structure and function. *Nature* *436*, 510–517.
- Stawicki, T.M., Zhou, K., Yochem, J., Chen, L., and Jin, Y. (2011). TRPM channels modulate epileptic-like convulsions via systemic ion homeostasis. *Curr. Biol.* *21*, 883–888.
- Tai, H.C., Besche, H., Goldberg, A.L., and Schuman, E.M. (2010). Characterization of the Brain 26S Proteasome and its Interacting Proteins. *Front. Mol. Neurosci.* *3*.
- Tulgren, E.D., Turgeon, S.M., Opperman, K.J., and Grill, B. (2014). The Nesprin family member ANC-1 regulates synapse formation and axon termination by functioning in a pathway with RPM-1 and  $\beta$ -Catenin. *PLoS Genet.* *10*, e1004481.
- Urbán, N., van den Berg, D.L., Forget, A., Andersen, J., Demmers, J.A., Hunt, C., Ayrault, O., and Guillemot, F. (2016). Return to quiescence of mouse neural stem cells by degradation of a proactivation protein. *Science* *353*, 292–295.
- van Roessel, P., Elliott, D.A., Robinson, I.M., Prokop, A., and Brand, A.H. (2004). Independent regulation of synaptic size and activity by the anaphase-promoting complex. *Cell* *119*, 707–718.
- Vandewalle, J., Langen, M., Zschätzsch, M., Nijhof, B., Kramer, J.M., Brems, H., Bauters, M., Lauwers, E., Srahna, M., Marynen, P., et al. (2013). Ubiquitin ligase HUWE1 regulates axon branching through the Wnt/ $\beta$ -catenin pathway in a *Drosophila* model for intellectual disability. *PLoS ONE* *8*, e81791.
- Vashlishan, A.B., Madison, J.M., Dybbs, M., Bai, J., Sieburth, D., Ch'ng, Q., Tavazoie, M., and Kaplan, J.M. (2008). An RNAi screen identifies genes that regulate GABA synapses. *Neuron* *58*, 346–361.
- Vincent, A., Briggs, L., Chatwin, G.F., Emery, E., Tomlins, R., Oswald, M., Middleton, C.A., Evans, G.J., Sweeney, S.T., and Elliott, C.J. (2012). parkin-induced defects in neurophysiology and locomotion are generated by metabolic dysfunction and not oxidative stress. *Hum. Mol. Genet.* *21*, 1760–1769.
- White, J.G., Southgate, E., Thomson, J.N., and Brenner, S. (1976). The structure of the ventral nerve cord of *Caenorhabditis elegans*. *Philos. Trans. R. Soc. Lond. B Biol. Sci.* *275*, 327–348.
- Yamada, T., Yang, Y., and Bonni, A. (2013). Spatial organization of ubiquitin ligase pathways orchestrates neuronal connectivity. *Trends Neurosci.* *36*, 218–226.
- Yao, I., Takagi, H., Ageta, H., Kahyo, T., Sato, S., Hatanaka, K., Fukuda, Y., Chiba, T., Morone, N., Yuasa, S., et al. (2007). SCRAPPER-dependent ubiquitination of active zone protein RIM1 regulates synaptic vesicle release. *Cell* *130*, 943–957.
- Yin, L., Joshi, S., Wu, N., Tong, X., and Lazar, M.A. (2010). E3 ligases Arf-bp1 and Pam mediate lithium-stimulated degradation of the circadian heme receptor Rev-erb  $\alpha$ . *Proc. Natl. Acad. Sci. USA* *107*, 11614–11619.
- Zhao, X., Heng, J.I., Guardavaccaro, D., Jiang, R., Pagano, M., Guillemot, F., lavarone, A., and Lasorella, A. (2008). The HECT-domain ubiquitin ligase Huwe1 controls neural differentiation and proliferation by destabilizing the N-Myc oncoprotein. *Nat. Cell Biol.* *10*, 643–653.
- Zhao, X., D'Arca, D., Lim, W.K., Brahmachary, M., Carro, M.S., Ludwig, T., Cardo, C.C., Guillemot, F., Aldape, K., Califano, A., et al. (2009). The N-Myc-DLL3 cascade is suppressed by the ubiquitin ligase Huwe1 to inhibit proliferation and promote neurogenesis in the developing brain. *Dev. Cell* *17*, 210–221.
- Zhen, M., and Jin, Y. (1999). The liprin protein SYD-2 regulates the differentiation of presynaptic termini in *C. elegans*. *Nature* *401*, 371–375.
- Zhen, M., and Samuel, A.D. (2015). *C. elegans* locomotion: small circuits, complex functions. *Curr. Opin. Neurobiol.* *33*, 117–126.
- Zhen, M., Huang, X., Bamber, B., and Jin, Y. (2000). Regulation of presynaptic terminal organization by *C. elegans* RPM-1, a putative guanine nucleotide exchanger with a RING-H2 finger domain. *Neuron* *26*, 331–343.
- Zoghbi, H.Y., and Bear, M.F. (2012). Synaptic dysfunction in neurodevelopmental disorders associated with autism and intellectual disabilities. *Cold Spring Harb. Perspect. Biol.* *4*.